

# Persistent $\text{Ca}^{2+}$ Current Contributes to a Prolonged Depolarization in *Aplysia* Bag Cell Neurons

Alan K. H. Tam, Julia E. Geiger, Anne Y. Hung, Chris J. Groten, and Neil S. Magoski

Department of Physiology, Queen's University, Kingston, Ontario, Canada

Submitted 28 July 2009; accepted in final form 8 October 2009

**Tam AK, Geiger JE, Hung AY, Groten CJ, Magoski NS.** Persistent  $\text{Ca}^{2+}$  current contributes to a prolonged depolarization in *Aplysia* bag cell neurons. *J Neurophysiol* 102: 3753–3765, 2009. First published October 14, 2009; doi:10.1152/jn.00669.2009. Neurons may initiate behavior or store information by translating prior activity into a lengthy change in excitability. For example, brief input to the bag cell neurons of *Aplysia* results in an approximate 30-min afterdischarge that induces reproduction. Similarly, momentary stimulation of cultured bag cell neurons evokes a prolonged depolarization lasting many minutes. Contributing to this is a voltage-independent cation current activated by  $\text{Ca}^{2+}$  entering during the stimulus. However, the cation current is relatively short-lived, and we hypothesized that a second, voltage-dependent persistent current sustains the prolonged depolarization. In bag cell neurons, the inward voltage-dependent current is carried by  $\text{Ca}^{2+}$ ; thus we tested for persistent  $\text{Ca}^{2+}$  current in primary culture under voltage clamp. The observed current activated between  $-40$  and  $-50$  mV exhibited a very slow decay, presented a similar magnitude regardless of stimulus duration (10–60 s), and, like the rapid  $\text{Ca}^{2+}$  current, was enhanced when  $\text{Ba}^{2+}$  was the permeant ion. The rapid and persistent  $\text{Ca}^{2+}$  current, but not the cation current, were  $\text{Ni}^{2+}$  sensitive. Consistent with the persistent current contributing to the response,  $\text{Ni}^{2+}$  reduced the amplitude of a prolonged depolarization evoked under current clamp. Finally, protein kinase C activation enhanced the rapid and persistent  $\text{Ca}^{2+}$  current as well as increased the prolonged depolarization when elicited by an action potential-independent stimulus. Thus the prolonged depolarization arises from  $\text{Ca}^{2+}$  influx triggering a cation current, followed by voltage-dependent activation of a persistent  $\text{Ca}^{2+}$  current and is subject to modulation. Such synergy between currents may represent a common means of achieving activity-dependent changes to excitability.

## INTRODUCTION

Activity-dependent mechanisms can alter neuronal membrane potential, responsiveness, or firing (Aizenman and Linden 2000; Eyzaguirre and Kuffler 1955; Nelson et al. 2005; Soto-Trevino et al. 2001; Tasaki et al. 1954). Some forms of short-term plasticity include plateau potentials and prolonged depolarizations, which follow a brief train of action potentials and may continue for seconds to minutes (Andrew and Dudek 1983; Rekling and Feldman 1997; Thompson and Smith 1976). These phenomena play key roles in motor pattern generation, neuroendocrine control, and learning and memory (Brown and Bourque 2004; Dembrow et al. 2004; Egorov et al. 2002; Russell and Hartline 1982; Teruyama and Armstrong 2005; Viana Di Prisco et al. 1997).

The bag cell neurons of the marine mollusk, *Aplysia californica*, initiate reproduction via a striking activity-dependent

change in excitability known as the afterdischarge (Kupfermann 1967; Kupfermann and Kandel 1970; Pinsker and Dudek 1977). Following transitory synaptic input, these neuroendocrine cells fire action potentials for around 30 min and secrete egg-laying hormone into the circulation (Chiu et al. 1979; Stuart et al. 1980). Analogous to the afterdischarge, a train of action potentials delivered to a cultured bag cell neuron evokes a prolonged depolarization that may be accompanied by spiking (Hung and Magoski 2007; Whim and Kaczmarek 1998). The prolonged depolarization is initially driven by a voltage-independent, nonselective cation current activated by  $\text{Ca}^{2+}$  influx during the train. Nevertheless, the cation current lasts only 3–5 min, whereas the depolarization extends for 15–30 min (Hung and Magoski 2007). The present study tests the hypothesis that a persistent  $\text{Ca}^{2+}$  current contributes to the maintenance of the prolonged depolarization.

Using *Aplysia* bursting neurons, Wilson and Wachtel (1974) first showed that regions of negative slope in the steady-state current-voltage relationship cause regenerative depolarization.  $\text{Ca}^{2+}$  current often provides the initial  $\text{Ca}^{2+}$  influx to activate a cation current that mediates inward current (Derjean et al. 2005; Fraser and MacVicar 1996; Gardam and Magoski 2009; Hasuo et al. 1990; Lupinsky and Magoski 2006; Wilson et al. 1996; Zhang et al. 1995). However, as originally found in *Helix* neurons by Eckert and Lux (1976), pacemaker current can also be attributed to the voltage-dependent activation of persistent  $\text{Ca}^{2+}$  current (Carlin et al. 2000b; Kononenko and Dudek 2006; Lee and Heckman 1998; Mercer et al. 2005; Russo and Hounsgaard 1996; Zhang and Harris-Warrick 1995).

We now demonstrate a complex interplay between  $\text{Ca}^{2+}$  and cation currents in generating the prolonged depolarization of *Aplysia* bag cell neurons. Opening of rapid voltage-dependent  $\text{Ca}^{2+}$  current during a train of action potentials results in  $\text{Ca}^{2+}$  influx, triggering a nonselective cation current and membrane depolarization; this activates a persistent voltage-dependent  $\text{Ca}^{2+}$  current to support the prolonged depolarization. Protein kinase C (PKC)-dependent upregulation of the  $\text{Ca}^{2+}$  current, which occurs during the afterdischarge in vivo (Wayne et al. 1999), enhances the prolonged depolarization. Interaction between voltage-independent and -dependent currents is profound and promotes the long-term changes in activity and excitability required for peptide release and reproductive behavior.

## METHODS

### *Animals and cell culture*

Adult *Aplysia californica* weighing 150–500 g were obtained from Marinus (Long Beach, CA) or Santa Barbara Marine Biologicals

Address for reprint requests and other correspondence: N. S. Magoski, Dept. of Physiology, Queen's University, 4th Floor, Botterell Hall, 18 Stuart St., Kingston, ON K7L 3N6, Canada (E-mail: magoski@queensu.ca).

(Santa Barbara, CA). Animals were housed in an approximate 300-l aquarium containing continuously circulating, aerated sea water (Instant Ocean, Aquarium Systems; Mentor, OH, or Kent sea salt, Kent Marine; Acworth, GA) at 14–16°C on a 12/12-h light/dark cycle and fed romaine lettuce five times per week.

For primary cultures of isolated bag cell neurons, animals were anesthetized by an injection of isotonic  $MgCl_2$  (around 50% body wt), and the abdominal ganglion was removed and incubated for 18 h at 22°C in neutral protease (13.33 mg/ml; 165859, Roche Diagnostics; Indianapolis, IN) dissolved in tissue culture artificial sea water (tcASW) composed of in mM: 460 NaCl, 10.4 KCl, 11  $CaCl_2$ , 55  $MgCl_2$ , 15 HEPES, 1 mg/ml glucose, 100 U/ml penicillin, and 0.1 mg/ml streptomycin, pH 7.8 with NaOH. The ganglion was then transferred to fresh tcASW, and the bag cell neuron clusters dissected from the surrounding connective tissue. Using a fire-polished Pasteur pipette and gentle trituration, neurons were dispersed onto 35 × 10-mm polystyrene tissue culture dishes (430165, Corning; Corning, NY) filled with 2 ml tcASW. Cultures were maintained in tcASW for 1–3 days in a 14°C incubator. Experiments were performed on neurons that were in vitro for ≥1 days. Salts were obtained from Fisher Scientific (Ottawa, ON, Canada) or Sigma (St. Louis, MO).

#### Whole cell, voltage-clamp recordings

Voltage-clamp recordings were made using an EPC-8 amplifier (HEKA Electronics; Mahone Bay, NS, Canada) and the tight-seal, whole cell method. Microelectrodes were pulled from 1.5 mm ID borosilicate glass capillaries (TW150F-4, World Precision Instruments; Sarasota, FL) and had a resistance of 1–2 MΩ when filled with either intracellular saline. Pipette junction potentials were nulled, and subsequent to seal formation, pipette capacitive currents were cancelled. Following break-through, neuronal capacitance was also cancelled, and the series resistance (3–5 MΩ) compensated to 80% and monitored throughout the experiment. Current was filtered at 1 kHz with the EPC-8 built-in Bessel filter and sampled at 2 kHz using a Digidata 1322A A/D converter (Axon Instruments/Molecular Devices; Sunnyvale, CA), a computer, and Clampex software (version 8.2, Axon Instruments). Voltage stimuli were delivered with either Clampex or a S88 stimulator (Grass; Warwick, MA).

$Ca^{2+}$  currents were isolated using  $Ca^{2+}$ - $Cs^+$ -TEA ASW, where the  $Na^+$  was replaced with TEA and the  $K^+$  with  $Cs^+$  (composition in mM: 460 TEA-Cl, 10.4 CsCl, 55  $MgCl_2$ , 11  $CaCl_2$ , and 15 HEPES, pH 7.8 with CsOH). The procedure also employed a  $Cs^+$ -aspartate-based intracellular saline with a composition (in mM) of 70 CsCl, 10 HEPES, 11 glucose, 10 glutathione, 5 ethyleneglycol bis (aminoethylether) tetraacetic acid (EGTA), 500 aspartic acid, 5 ATP (grade 2, disodium salt; A3377, Sigma), and 0.1 GTP (type 3, disodium salt; G8877, Sigma), pH 7.3 with CsOH.  $Ba^{2+}$  currents were isolated in the same manner, with the exception of the external containing 460 mM TEA-Br instead of TEA-Cl and 11 mM  $BaCl_2$  instead of  $CaCl_2$ . On-line leak subtraction for rapid, voltage-gated  $Ca^{2+}$  currents involved a P/4 protocol from –60 or –90 mV with subpulses of opposite polarity and one-fourth the magnitude, an inter-subpulse interval of 500 ms, and 100 ms before actual test pulses of 200 ms. Persistent  $Ca^{2+}$  currents were measured by delivering voltage steps (10-s, 30-s, or 1-min duration) before and after block by 10 mM  $Ni^{2+}$  ( $NiCl_2$ ; N6136, Sigma), then subtracting the current in  $Ni^{2+}$  from that under control. A junction potential of 20 mV was compensated for by subtraction off-line in both rapid and persistent current measurements.

The prolonged depolarization current ( $I_{PD}$ ) was elicited by a 5-Hz train of 100-ms voltage steps from –60 to +10 mV for 10 s (see RESULTS for details) under whole cell voltage-clamp with normal ASW (nASW; composition as per tcASW with the glucose, penicillin, and streptomycin omitted) in the bath and regular intracellular solution (composition in mM: 500  $K^+$ -aspartate, 70 KCl, 1.25  $MgCl_2$ , 10 HEPES, 11 glucose, 10 glutathione, 5 ATP, and 0.1 GTP; pH 7.3 with

KOH) in the pipette. A junction potential of 15 mV was compensated for by subtraction off-line.

#### Sharp-electrode, current-clamp recordings

Current-clamp recordings were made in nASW using an AxoClamp 2B (Axon Instruments) amplifier and the sharp-electrode bridge-balanced method. Microelectrodes were pulled from 1.2 mm ID borosilicate glass capillaries (TW120F-4, World Precision Instruments) and had a resistance of 5–20 MΩ when filled with 2 M  $K^+$ -acetate plus 10 mM HEPES and 100 mM KCl (pH = 7.3 with KOH). Current was delivered with either Clampex or the S88 stimulator. Voltage was filtered at 3 kHz using the Axoclamp built-in Bessel filter and sampled at 2 kHz as per current.

#### $Ca^{2+}$ imaging

The  $Ca^{2+}$ -sensitive dye, fura-PE3 ( $K^+$  salt, 0110; Teflabs, Austin, TX) (Vorndran et al. 1995), was injected using a PMI-100 pressure microinjector (Dagan, Minneapolis, MN), while simultaneously monitoring membrane potential with the Axoclamp. Microelectrodes (as per sharp-electrode current clamp) had a resistance of 15–30 MΩ when tip-filled with 10 mM fura-PE3 and backfilled with 3 M KCl. Filling neurons with an optimal amount of dye, estimated at 50–100  $\mu M$ , required 3–10 300- to 900-ms pulses at 50–100 kPa. After injection, neurons were allowed to equilibrate for ≥30 min. Imaging was performed in nASW using a Nikon TS100-F inverted microscope (Nikon, Mississauga, ON, Canada) equipped with Nikon Plan Fluor ×60 (NA = 0.7) or ×100 (NA = 1.3) objective while under simultaneous voltage clamp. The light source was a 75-W Xenon arc lamp and a multi-wavelength DeltaRAM V monochromatic illuminator (Photon Technology International, London, ON, Canada) coupled to the microscope with a UV-grade liquid-light guide. Excitation wavelengths of 340 and 380 nm were controlled by a Photon Technology International computer interface, a computer, and ImageMaster Pro software (version 1.49, Photon Technology International). Emitted light passed through a 510/40-nm barrier filter prior to being detected by a Photon Technology International IC200 intensified charge coupled device camera. The camera black level was set prior to an experiment such that at a gain of 1, and with no light going to the camera, there was a 50:50 distribution of blue and black pixels on the image display. The camera intensifier voltage was set based on the initial fluorescence intensity of a neuron at the start of the experiment and maintained constant thereafter. Fluorescence intensities were sampled every 10 s from regions of interests (ROIs) defined over the soma and averaged four to eight frames per acquisition. The emission following 340 and 380 nm excitation was ratioed (340/380) to reflect free intracellular  $Ca^{2+}$  and saved for subsequent analysis. Black level adjustment, image acquisition, frame averaging, emitted light ROI sampling, and ratio calculations were performed by ImageMaster Pro.

#### Reagents and drug application

In cases where  $Ni^{2+}$  was used to subtract leak current, it was applied via a gravity-driven perfusion system before the stimulus was given. In experiments where  $Ni^{2+}$  was applied after a prolonged depolarization was elicited under sharp-electrode current clamp, it was perfused following the stimulus. Dimethyl sulfoxide (DMSO; BP231-1, Fisher) was used as the vehicle for phorbol 12-myristate 13-acetate (PMA; P8139, Sigma). Bag cell neurons were pretreated for 20–30 min in 0.5% DMSO or 100 nM PMA.

#### Analysis

The current-voltage relationship of rapid  $Ca^{2+}$  or  $Ba^{2+}$  current was ascertained using Clampfit software (version 8.2, Axon Instru-

ments) by measuring peak current between cursors set as close as possible to the start and end of leak-subtracted traces. Current was normalized to cell size by dividing by neuronal capacitance (obtained from the EPC-8 whole cell capacitance compensation circuitry) and plotted against voltage. Activation curves were determined by dividing the current elicited at each voltage step by the maximum current elicited during the protocol (+10 mV; see RESULTS for details). This was averaged across cells at a given step voltage, plotted against that voltage, and fit with a Boltzmann equation in Origin (version 7, OriginLab; Northampton, MA). Pseudo-steady-state inactivation curves were determined by first delivering a 10-s inactivating step, then testing the current by stepping to +10 mV and subsequently dividing all test currents by the maximal test current (evoked from an inactivation step of -90 or -60; see RESULTS for details). This was averaged across cells at a given inactivating voltage, plotted against that voltage, and again fit with a Boltzmann. The fits provided the half-maximal voltage ( $V_{1/2}$ ) of activation (the voltage required to recruit half of the maximum current) or inactivation (the voltage at which half of the current remains for recruitment) and the slope factor ( $k$ ; the amount of voltage required to change the current  $e$ -fold).

The current-voltage relationship of persistent  $\text{Ca}^{2+}$  or  $\text{Ba}^{2+}$  currents was also established using Clampfit. Following leak subtraction by  $\text{Ni}^{2+}$  block, cursors were placed at the beginning and end of the period in the current trace prior to stimulus application, and the mean between these two cursors was taken as the holding current. Cursors were also placed near the end of the voltage step, separated by either 1 s for the 10- and 30-s steps or 10 s for the 1-min steps. The mean between these two cursors was taken as the current elicited by the step. The difference between the mean current during the step and the mean holding current was taken as the persistent current. Current was normalized to cell size by dividing by the whole cell capacitance and plotted against step voltage.

Clampfit was used to determine peak amplitude of either an evoked depolarization or  $I_{\text{PD}}$ . Cursors were placed at baseline voltage or current, prior to delivery of the stimulus, as well as at peak voltage or current amplitude during or after the stimulus. The difference between the two cursor values was taken as the amplitude. The prolonged depolarization current was normalized to cell capacitance. For display, voltage traces and  $I_{\text{PD}}$  were filtered off-line to 10–20 Hz using Clampfit. The very slow nature of the membrane potential responses as well as  $I_{\text{PD}}$  ensured that no change in amplitude or kinetics was brought about by this second filtering.

For intracellular  $\text{Ca}^{2+}$ , Origin was used to import and plot ImageMaster Pro files as line graphs. The steady-state value of the baseline 340/380 ratio under simultaneous voltage clamp at -60 mV was compared with the ratio from regions that had reached a peak or new steady state during a 1-min step to a depolarized potential. Averages of both regions were determined by eye or with adjacent-averaging. Change was expressed as a percent change (% change 340/380) of the new ratio over the baseline ratio.

Data are presented as the means  $\pm$  SE as calculated using either Origin or Instat (version 3.05; GraphPad Software; San Diego, CA). Statistical analysis was performed using Instat. The Kolmogorov-Smirnov method was used to test data sets for normality. A one-sample  $t$ -test was used to determine if the mean of a single group was different from a mean of zero. Student's paired or unpaired  $t$ -test (with the Welch correction as required) or the Mann-Whitney test was used to compare differences between two means, while either a standard one-way ANOVA and the Student-Newman-Keuls multiple-comparisons post hoc test or a Kruskal-Wallis nonparametric ANOVA and Dunn's multiple comparisons post hoc test were used to compare differences between multiple means. Means were considered significantly different if the  $P$  value was  $<0.05$ .

## RESULTS

### Rapid voltage-gated $\text{Ca}^{2+}$ current in cultured bag cell neurons

Bag cell neuron  $\text{Ca}^{2+}$  current has been examined previously (Conn et al. 1989; DeRiemer et al. 1985b; Hung and Magoski 2007; Zhang et al. 2008); however, the information on permeation and fundamental biophysics is less than complete (Fieber 1995). Employing a  $\text{Cs}^+$ -aspartate-based intracellular saline and  $\text{Ca}^{2+}$ - $\text{Cs}^+$ -TEA ASW in the bath, cultured bag cell neurons were whole cell voltage-clamped at -60 mV and  $\text{Ca}^{2+}$  currents evoked with 200-ms square pulses from -60 to +40 mV in 10-mV increments. What we designate here as the rapid  $\text{Ca}^{2+}$  current was fast activating, strongly voltage-dependent, moderately inactivating during the pulse, and maximal at +10 mV (Fig. 1A, left). As our laboratory has demonstrated previously (Hung and Magoski 2007), these currents were abolished by 10 mM of the general  $\text{Ca}^{2+}$  channel blocker,  $\text{Ni}^{2+}$  (Byerly et al. 1985; McFarlane and Gilly 1998) (Fig. 1A, right). Compared with control ( $n = 9$ ), there was an absence of inward current at all voltages following  $\text{Ni}^{2+}$  block ( $n = 6$ ) (Fig. 1B). In certain subsequent experiments, we used 10 mM  $\text{Ni}^{2+}$  to block  $\text{Ca}^{2+}$  currents under voltage or current clamp.

$\text{Ca}^{2+}$  channels are permeable to other divalent cations, such as  $\text{Ba}^{2+}$  (Hagiwara et al. 1974; Hille 2001). Substituting  $\text{Ba}^{2+}$  for  $\text{Ca}^{2+}$  typically results in larger currents and in some instances a negative shift in the  $V_{1/2}$  voltage of activation (Byerly et al. 1985; Hess et al. 1986).  $\text{Ba}^{2+}$  currents were recorded as per  $\text{Ca}^{2+}$  currents, but with  $\text{Ba}^{2+}$ - $\text{Cs}^+$ -TEA ASW externally. Particularly at test potentials more negative than 0 mV, the  $\text{Ba}^{2+}$  current was larger than the  $\text{Ca}^{2+}$  current ( $n = 7$ ; Fig. 1C). Contributing to this apparent increase in amplitude was a negative shift in the peak  $\text{Ba}^{2+}$  current to 0 mV (Fig. 1D). The latter result lead us to consider the possibility that replacing  $\text{Ca}^{2+}$  with  $\text{Ba}^{2+}$  as a charge carrier may have altered the voltage dependence of activation and/or inactivation, an observation we have made previously when studying cation channels (Geiger et al. 2009).

For activation, both  $\text{Ca}^{2+}$  and  $\text{Ba}^{2+}$  currents were normalized to the current evoked during the pulse to +10 mV and plotted against test pulse voltage. A Boltzmann fit of these relationships showed a left-shifted activation with  $\text{Ba}^{2+}$  as indicated by the more negative  $V_{1/2}$  of activation (about -6 mV in  $\text{Ca}^{2+}$  vs. about -19 mV in  $\text{Ba}^{2+}$ ;  $n = 8$  and 7; Fig. 2A). The  $k$  values reflected a small increase in sensitivity with  $\text{Ba}^{2+}$  (near 5 in  $\text{Ca}^{2+}$  vs. near 4 in  $\text{Ba}^{2+}$ ). For steady-state inactivation, neurons were held at either -60 mV (for  $\text{Ca}^{2+}$ ) or -90 mV (for  $\text{Ba}^{2+}$ ), and prior to a +10-mV test pulse, currents were inactivated with 10-s steps to +10 mV in 10-mV increments. Fitting a Boltzmann function to the inactivation curves revealed that  $\text{Ba}^{2+}$  currents ( $n = 8$ ) inactivated at a more hyperpolarized voltage compared with  $\text{Ca}^{2+}$  currents ( $n = 5$ ; Fig. 2B). This was reflected by the more negative  $V_{1/2}$  of inactivation (around -14 in  $\text{Ca}^{2+}$  vs. around -30 in  $\text{Ba}^{2+}$ ) and was accompanied by a slight increase in sensitivity with a lowering of the  $k$  value ( $\sim 10$  in  $\text{Ca}^{2+}$  vs.  $\sim 8$  in  $\text{Ba}^{2+}$ ). For simultaneous comparison of activation and inactivation, the curves derived from the Boltzmann fits of the  $\text{Ca}^{2+}$  current are re-plotted in Fig. 2C. A reasonable degree of overlap was evident between the two curves with a point of intersection at close to -9 mV.

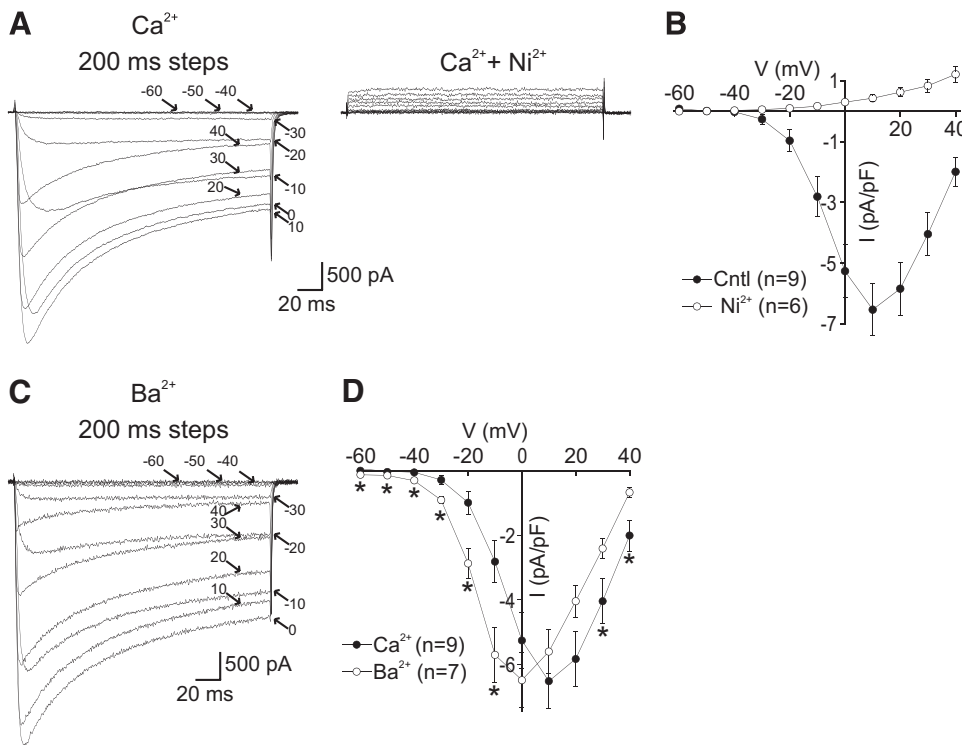


FIG. 1. Rapid voltage-activated  $\text{Ca}^{2+}$  current in cultured bag cell neurons. **A**, *left*: traces of  $\text{Ca}^{2+}$  currents evoked with 200-ms square pulses from  $-60$  to  $+40$  mV in  $10$ -mV increments as indicated.  $\text{Ca}^{2+}$  currents are isolated with  $\text{Ca}^{2+}$ - $\text{Cs}^+$ -TEA artificial seawater (ASW) and  $\text{Cs}^+$ -aspartate intracellular solution. *Right*: traces of currents evoked under the same conditions, except following the addition of  $10$  mM  $\text{Ni}^{2+}$ . Scale bars apply to both panels. **B**: summary of peak current, with and without  $\text{Ni}^{2+}$ , normalized to capacitance and plotted versus the step voltages from **A**. The current following  $\text{Ni}^{2+}$  block is small ( $\circ$ ), relative to the peak  $\text{Ca}^{2+}$  current ( $\bullet$ ). **C**: traces of  $\text{Ba}^{2+}$  currents isolated with  $\text{Ba}^{2+}$ - $\text{Cs}^+$ -TEA ASW and evoked as indicated with  $200$ -ms square pulses from  $-60$  to  $+40$  mV in  $10$ -mV increments. **D**: summary of peak  $\text{Ba}^{2+}$  ( $\circ$ ) or  $\text{Ca}^{2+}$  ( $\bullet$ ; re-plotted from **B**) current normalized to capacitance. Average currents carried by  $\text{Ba}^{2+}$  are significantly larger at all negative test potentials and significantly smaller at the most positive test potentials ( $*P < 0.05$ , 2-tailed unpaired Student's  $t$ -test; Welch corrected for  $-60$ ,  $-50$ ,  $-40$ ,  $+30$ , and  $+40$  mV).

### Persistent voltage-gated $\text{Ca}^{2+}$ current in cultured bag cell neurons

The prolonged depolarization in bag cell neurons is driven by a voltage-independent, nonselective cation current that lasts for 3–5 min under voltage clamp (Hung and Magoski 2007). Because the prolonged depolarization lasts upward of 30 min, we hypothesized that the response is maintained by a persistent voltage-dependent  $\text{Ca}^{2+}$  current. To test this, cultured bag cell neurons were voltage-clamped at  $-60$  mV and stimulated in  $10$ -mV increments with  $10$ - or  $30$ -s square pulses to  $-20$  mV ( $n = 7$  and  $5$ ; Fig. 3, **A** and **B**) or  $1$ -min pulses to  $-30$  mV ( $n = 6$ ; 3C). Currents were leak subtracted by delivering the voltage steps before and after  $10$  mM  $\text{Ni}^{2+}$  block, then subtracting the current in  $\text{Ni}^{2+}$  from that under control. During all steps,  $\text{Ni}^{2+}$  eliminated much of the current, but subtraction revealed a small, inward, voltage-dependent current after any fast, partial inactivation at the onset of the step. Particularly over the  $1$ -min pulse, the current was essentially stable throughout. Mean currents taken near the end of the step (see METHODS for details) were not significantly different between the three durations at a given voltage except for the step to  $-50$  mV for  $10$  s versus  $30$  s or  $1$  min (Fig. 3D).

As an independent assessment of  $\text{Ca}^{2+}$  entry under more physiological conditions, fura-loaded cultured bag cell neurons were ratiometrically imaged in nASW while simultaneously voltage-clamped at  $-60$  mV. Delivery of  $1$ -min step depolarizations from  $-50$  to  $-20$  mV in  $10$ -mV increments induced clear elevations of intracellular  $\text{Ca}^{2+}$  as indicated by an increase in the  $340/380$  fura-PE3 ratio ( $n = 17$ ; Fig. 4A). Changes in  $\text{Ca}^{2+}$  were most prominent, although more transitory, during pulses to  $-30$  and  $-20$  mV; however, depolarization to  $-40$  and even  $-50$  mV elicited resolvable  $\text{Ca}^{2+}$  increases. The mean change in  $\text{Ca}^{2+}$  evoked by stepping to  $-20$  mV was significantly different from that produced by

pulses to  $-50$  or  $-40$  mV; this was also the case for the step to  $-30$  mV compared with  $-50$  mV (Fig. 4B). Overall there was a clear nonlinear trend for greater intracellular  $\text{Ca}^{2+}$  with greater depolarization, indicative of voltage-gating mediating the response. These data suggest that in a normal ionic environment, even relatively small alterations to membrane potential can permit  $\text{Ca}^{2+}$  entry.

Given that the rapid current was relatively larger over the negative range of test voltages with  $\text{Ba}^{2+}$  substituted for  $\text{Ca}^{2+}$  (see Fig. 1D), we examined the persistent current using  $\text{Ba}^{2+}$  as a charge carrier. Because there was relatively little difference between  $\text{Ca}^{2+}$  currents at the three extended test pulse durations (see Fig. 3D), we used the  $10$ -s step duration in this and subsequent experiments. Cultured bag cell neurons were stimulated from a holding potential of  $-60$  to  $-20$  mV in  $10$ -mV increments under voltage clamp (Fig. 5A). Once normalized to cell capacitance, the mean  $\text{Ba}^{2+}$  current ( $n = 7$ ) was larger when compared with  $\text{Ca}^{2+}$  current ( $n = 6$ ) recorded in separate experiments, with the difference reaching significance at  $-30$  and  $-20$  mV (Fig. 5B). This indicates the persistent current, like the rapid current, resembles a typical  $\text{Ca}^{2+}$  channel and shows a greater conductance with  $\text{Ba}^{2+}$  as the permeating ion.

### $\text{Ni}^{2+}$ does not inhibit the prolonged depolarization current but attenuates the prolonged depolarization itself

Hung and Magoski (2007) demonstrated that the initial current driving the prolonged depolarization ( $I_{\text{PD}}$ ) was a voltage-independent nonselective cation channel. It is unlikely that the persistent  $\text{Ca}^{2+}$  current contributes directly to  $I_{\text{PD}}$ ; nevertheless, we tested this possibility by attempting to block  $I_{\text{PD}}$  with  $\text{Ni}^{2+}$ . As per Hung and Magoski (2007),  $I_{\text{PD}}$  was evoked in cultured bag cell neurons voltage-clamped at  $-60$  mV in nASW with a  $\text{K}^+$ -aspartate-based intracellular solution using a

5-Hz, 10-s train of 100-ms pulses to +10 mV ( $n = 5$ ; Fig. 6A, left). This stimulus is analogous in frequency and duration to the train of synaptic input delivered to the intact cluster when triggering an afterdischarge (Kaczmarek et al. 1982; Magoski and Kaczmarek 2005). The posttrain current was similar to what we have reported previously, i.e., relatively slow onset with a near complete decay over the course of 10 min. This current was compared with  $I_{PD}$  elicited from different cells but with 10 mM  $\text{Ni}^{2+}$  perfused onto the neuron just after the train

( $n = 5$ ; Fig. 6A, right). The data showed that  $\text{Ni}^{2+}$  did not block  $I_{PD}$ , leaving the peak amplitude unchanged (Fig. 6B).

We used the fact that  $\text{Ni}^{2+}$  does not block  $I_{PD}$  to evaluate whether the persistent  $\text{Ca}^{2+}$  current plays a role in the maintenance of the prolonged depolarization after  $I_{PD}$  has diminished. Again as per Hung and Magoski (2007), prolonged depolarizations were evoked from cultured bag cell neurons under current clamp in nASW with a  $\text{K}^+$ -acetate-filled sharp electrode using a 5-Hz, 10-s train of action potentials. Once a depolarization had plateaued, 10 mM  $\text{Ni}^{2+}$  was added to the bath ( $n = 8$ ; Fig. 7A). Perfusion of  $\text{Ni}^{2+}$  led to a relatively rapid reduction of the prolonged depolarization magnitude with a near 75% percent recovery back to baseline (-60 mV) that reached the level of significance compared with a mean of zero (Fig. 7B).

Our study employed  $\text{Ni}^{2+}$  as a general  $\text{Ca}^{2+}$  channel blocker; however,  $\text{Ni}^{2+}$  also specifically blocks low-voltage-activated/T-type  $\text{Ca}^{2+}$  currents when used at comparatively low concentrations, including in the related mollusk, *Lymnaea* (Fox et al. 1987; Lee et al. 1999; Yeoman et al. 1999). Based on biophysics, it is unlikely that a T-type  $\text{Ca}^{2+}$  current is involved in the generation or maintenance of the prolonged depolarization. In particular, T-type channels inactivate at voltages equivalent or more positive than resting potential, and when activated, they turn off in <200 ms (Carbone and Lux 1984; Fox et al. 1987). Nevertheless, to ensure that T-type  $\text{Ca}^{2+}$  current was not present, cultured bag cell neurons were again voltage-clamped using  $\text{Cs}^+$ -aspartate-based intracellular saline and  $\text{Ca}^{2+}$ - $\text{Cs}^+$ -TEA ASW in the bath.  $\text{Ca}^{2+}$  currents were evoked with 200-ms square pulses from -60 to +40 mV in 10-mV increments from either a control holding potential of -60 mV ( $n = 10$ ) or, to remove inactivation of any potential T-type current, -90 mV ( $n = 8$ ). Consistent with an absence of T-type  $\text{Ca}^{2+}$  channels, the current-voltage relationships obtained from the two holding potentials were virtually identical (Fig. 7C). If a low-voltage-activated current was expressed, there would have been a distinct plateau in the relationship somewhere between -60 and -20 mV (Carbone and Lux 1984).

The block of an ongoing prolonged depolarization by  $\text{Ni}^{2+}$  suggests the persistent  $\text{Ca}^{2+}$  current plays a role in maintaining the response, but it does not provide information as to which current is at work during the initial phase. In an attempt to address this, prolonged depolarizations were elicited in control neurons ( $n = 8$ ) versus cells that

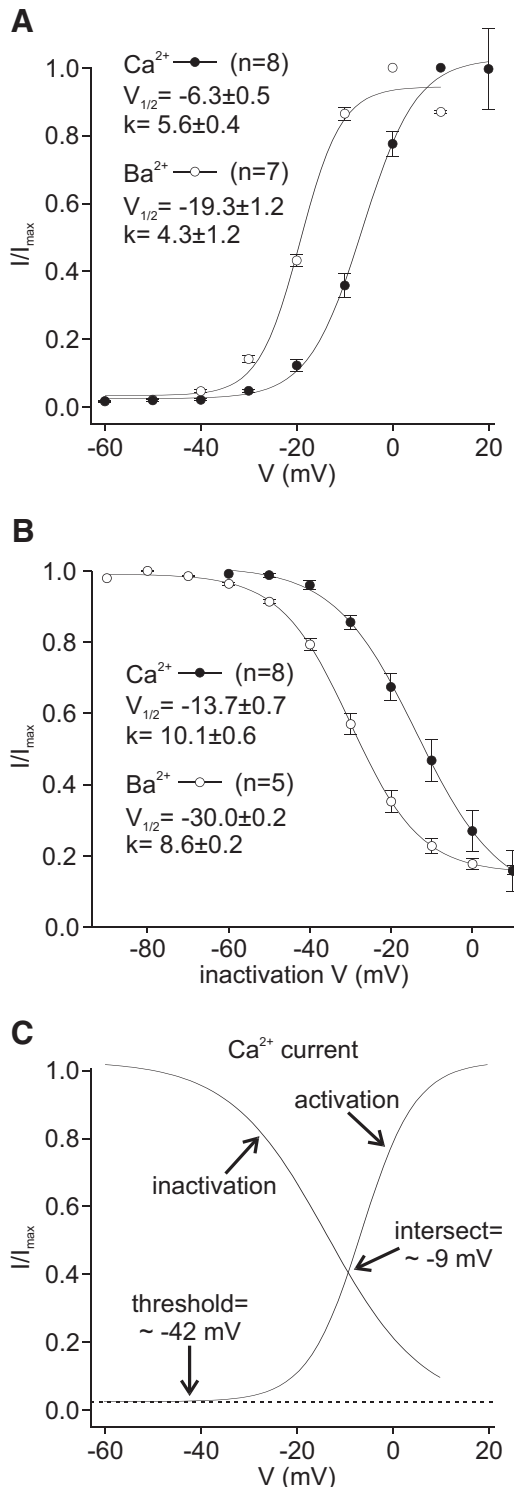


FIG. 2. Activation and inactivation characteristics of rapid  $\text{Ca}^{2+}$  and  $\text{Ba}^{2+}$  currents. **A**: activation curves for  $\text{Ca}^{2+}$  and  $\text{Ba}^{2+}$  current. Currents are normalized to maximum current, plotted against voltage, and fit with a Boltzmann function. The activation curve with  $\text{Ba}^{2+}$  is shifted left as indicated by the lower  $V_{1/2}$ , but there is little change in sensitivity, as reflected by similar  $k$  values. **B**: steady-state inactivation curves for  $\text{Ca}^{2+}$  and  $\text{Ba}^{2+}$  current. From a holding potential of either -60 mV (for  $\text{Ca}^{2+}$ ) or -90 mV (for  $\text{Ba}^{2+}$ ), the current is inactivated with a 10-s step to +10 mV in 10-mV increments followed by a 200-ms test pulse to +10 mV. The steady-state current evoked during each test pulse is divided by the maximal test pulse current (elicited from -60 or -90 mV for  $\text{Ca}^{2+}$  and  $\text{Ba}^{2+}$ ), plotted against the corresponding inactivation step voltage, and fit with a Boltzmann function.  $\text{Ba}^{2+}$  inactivates at a more hyperpolarized voltage compared with  $\text{Ca}^{2+}$ , indicated by its lower  $V_{1/2}$ , and is somewhat more sensitive, as reflected by the lower  $k$  value. **C**: a re-plot of the  $\text{Ca}^{2+}$  current activation and inactivation curves, provided by the Boltzmann fit, on the same graph and at the same scale. The data points are removed for clarity. The activation curve shows a threshold of around -42 mV and intersects with the inactivation curve near -9 mV. Overlap between the 2 curves was evident, particularly between -40 and 0 mV.

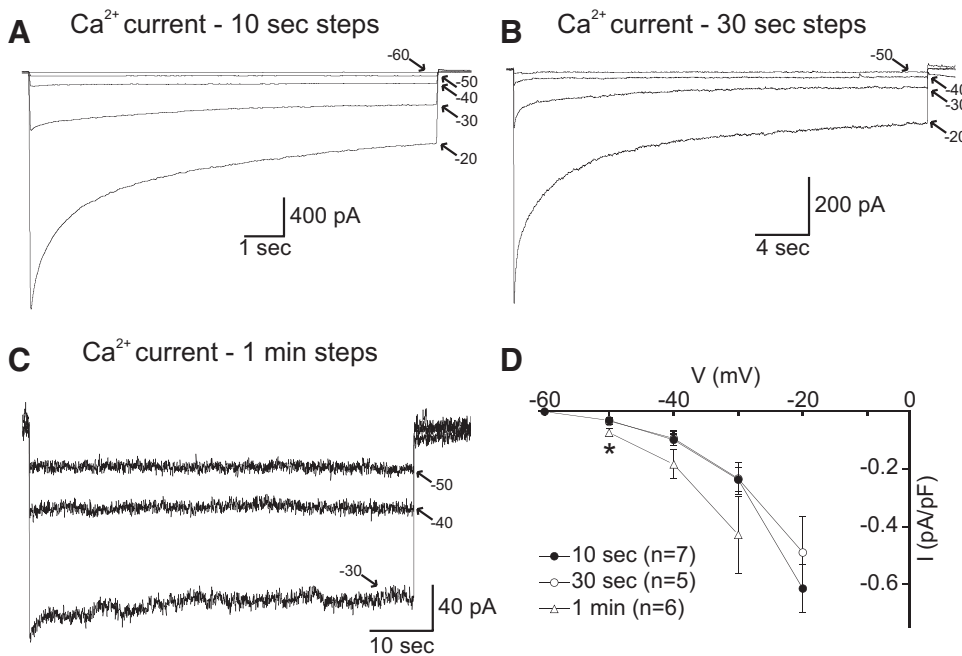


FIG. 3. Persistent voltage-activated  $\text{Ca}^{2+}$  current in cultured bag cell neurons. **A** and **B**: traces of  $\text{Ca}^{2+}$  currents evoked by 10- or 30-s square pulses from a holding potential of  $-60$  to  $-20$  mV in 10-mV increments. Currents are resolved by delivering the voltage steps before and after 10 mM  $\text{Ni}^{2+}$  block, then subtracting the current in  $\text{Ni}^{2+}$  from that under control. **C**: traces of  $\text{Ca}^{2+}$  currents evoked by 1-min square pulses from a holding potential of  $-60$  to  $-30$  mV in 10-mV increments. Again,  $\text{Ni}^{2+}$  subtraction is used to remove the leak. **D**: summary graph of mean persistent  $\text{Ca}^{2+}$  current normalized to cell capacitance. The persistent current is measured as the mean of the last 1 s during the 10- and 30-s steps or the last 10 s of the 1-min step. Mean currents are not significantly different, except at  $-50$  mV between the 10-s and 1-min step, as well as between the 30-s and 1-min step ( $*P < 0.05$ , 1-way ANOVA, Student-Newman-Keuls multiple comparison post hoc test).

were exposed to 10 mM  $\text{Ni}^{2+}$  immediately after the 5-Hz, 10-s train of action potentials ( $n = 8$ ) (Fig. 7D). In both cases, the depolarization was evident and the difference between the two conditions did not reach significance (control:  $9.8 \pm 4.4$  mV vs.  $\text{Ni}^{2+}$ :  $10.5 \pm 3.0$  mV;  $P > 0.05$ , 2-tailed unpaired Student's *t*-test). However, delivery of  $\text{Ni}^{2+}$  prior to development of the prolonged depolarization shortened the duration of the response. Compared with control,  $\text{Ni}^{2+}$ -exposed neurons largely recovered to the pre-stimulus membrane potential within 10 min (control:  $16.3 \pm 12.5\%$  recovery vs.  $\text{Ni}^{2+}$ :  $96.4 \pm 3.6\%$  recovery;  $P < 0.01$ , Mann-Whitney test). This is consistent with the cation channel being capable of depolarizing the neurons at the start of the response but nevertheless requiring subsequently recruitment of the  $\text{Ca}^{2+}$  current to keep the voltage depolarized.

#### PKC activation enhances both rapid and persistent $\text{Ca}^{2+}$ current

It is established that activation of PKC augments bag cell neuron  $\text{Ca}^{2+}$  current (Conn et al. 1989; DeRiemer et al. 1985b; Strong et al. 1987; Zhang et al. 2008). Moreover, PKC activity is elevated shortly after the onset of the afterdischarge in intact bag cell neuron clusters (Wayne et al. 1999). We confirmed the effect of PKC on rapid  $\text{Ca}^{2+}$  currents evoked in cultured bag cell neurons with 200-ms square pulses from  $-60$  to  $+40$  mV in 10-mV increments following 30-min pretreatment in the vehicle, 0.1% DMSO ( $n = 9$ ) or 100 nM of the PKC-activating phorbol ester, PMA ( $n = 8$ ) (Castagna et al. 1982; DeRiemer et al. 1985a; Manseau et al. 2001). As expected, upregulation of PKC caused a marked enhancement of  $\text{Ca}^{2+}$  current compared with control (Fig. 8A, left and middle). The difference in

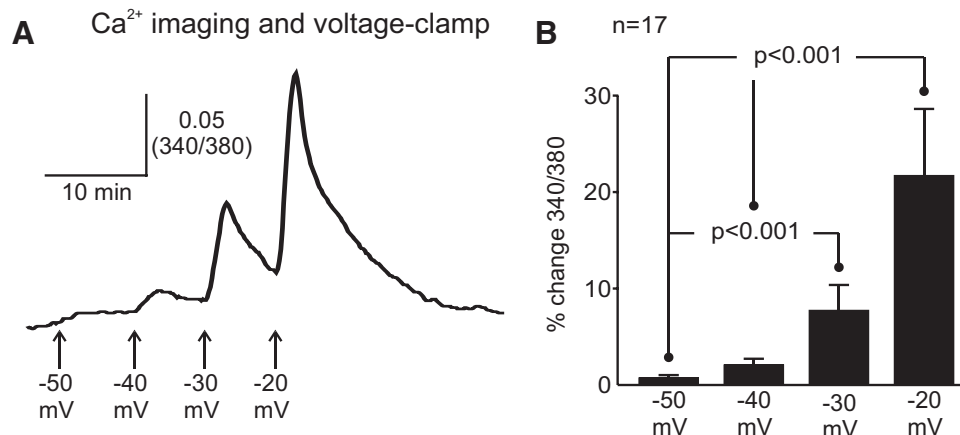


FIG. 4. Modest depolarizations elevate intracellular  $\text{Ca}^{2+}$  in cultured bag cell neurons. **A**: sample of intracellular  $\text{Ca}^{2+}$  as measured by 340/380 nm imaging of a fura PE3-loaded neuron bathed in nASW and simultaneously voltage-clamped at  $-60$  mV.  $\text{Ca}^{2+}$  influx is evoked by 1-min square pulses to  $-50$  mV through  $-20$  mV in 10-mV increments as indicated. While the response is more long-lasting at  $-50$  or  $-40$  mV, stepping to  $-30$  or  $-20$  mV reliably produces a prominent peak of  $\text{Ca}^{2+}$  influx that subsequently decays. **B**: grouped imaging data of peak percentage change shows that intracellular  $\text{Ca}^{2+}$  increases in nonlinear manner as the membrane potential is made more positive, consistent with an underlying voltage-dependent process. Compared with the mean change during the  $-50$ -mV step, the responses reach the level of significance when the membrane potential is changed to  $-30$  or  $-20$  mV; in addition, the mean change at  $-40$  mV is significantly different from that at  $-20$  mV (Kruskal-Wallis nonparametric ANOVA, Dunn's multiple comparison post hoc test).

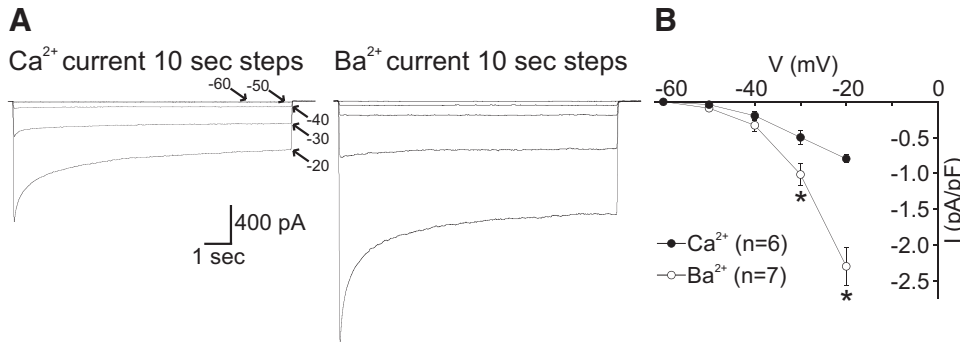


FIG. 5. The persistent current is larger when  $\text{Ba}^{2+}$  is the charge carrier. *A*: traces of  $\text{Ca}^{2+}$  (left) or  $\text{Ba}^{2+}$  (right) currents evoked by 10-s square pulses from a holding potential of  $-60$  to  $-20$  mV in 10-mV increments. The  $\text{Ba}^{2+}$  current is typically larger than the  $\text{Ca}^{2+}$  current. Scale bars apply to both panels. *B*: summary graph of mean persistent  $\text{Ca}^{2+}$  and  $\text{Ba}^{2+}$  current. Current is measured as the mean of the last 1 s and normalized to cell capacitance. The difference in persistent current between  $\text{Ca}^{2+}$  and  $\text{Ba}^{2+}$  is significant at  $-30$  and  $-20$  mV ( $*P < 0.05$ , 2-tailed unpaired Student's *t*-test; Welch corrected for  $-20$  mV).

average peak current, normalized to cell capacitance, between the two conditions was significant at all voltages except  $-60$ ,  $-50$ , and  $+40$  mV (Fig. 8*A*, right).

We next examined if the persistent current in those same PMA-responsive neurons also shared a sensitivity to PKC-dependent modulation. To test this, persistent  $\text{Ca}^{2+}$  currents were evoked by 10-s square pulses from  $-60$  to  $-20$  mV in 10-mV increments. The results showed that the presence of PMA lead to a larger persistent current (Fig. 8*B*, left and middle). The difference in the mean end-pulse current, normalized for cell size, reached the level of significance at  $-30$  and  $-20$  mV (Fig. 8*B*, right).

*PKC activation does not alter the prolonged depolarization elicited by an action potential train*

Knowing that the persistent  $\text{Ca}^{2+}$  current plays a role in the maintenance of the prolonged depolarization and this current is PKC sensitive, it follows that the prolonged depolarization should be PKC sensitive. This was examined by evoking the prolonged depolarization in current clamp with a 5-Hz, 10-s train of action potentials following 20-min pretreatment with 0.1% DMSO ( $n = 9$ ) or 100 nM PMA ( $n = 9$ ). Interestingly, the prolonged depolarization elicited under either condition was essentially the same ( $\sim 10$ – $12$  mV; Fig. 9*A*). The difference in the average depolarization between the two groups was not significant (Fig. 9*B*). Our laboratory previously found that induction of either  $I_{PD}$  or the prolonged depolarization was actually limited or decreased when  $\text{Ca}^{2+}$  influx during the train was too great (Hung and Magoski 2007). Thus it is not surprising that following the PKC-induced enhancement of the rapid  $\text{Ca}^{2+}$  current, the prolonged depolarization remained unchanged even though the persistent current would also be

augmented. Moreover, there is the issue of how PKC activation is timed. In the intact cluster, PKC would be upregulated subsequent to the delivery of the stimulus (Wayne et al. 1999), whereas our experimental conditions necessitate that PKC be turned on by PMA prior to the train.

*PKC activation enhances the prolonged depolarization elicited by a current ramp mimicking  $I_{PD}$*

To avoid the confounding issue of PKC over-enhancing  $\text{Ca}^{2+}$  influx during the initiation of the prolonged depolarization, as well as any unknown effects on  $I_{PD}$ , the response was instead elicited in a manner that did not involve a train of action potentials. Specifically, a current ramp approximating an average  $I_{PD}$ , i.e., an inverted version of the inward current observed under voltage clamp, was delivered to cultured bag cell neurons under current clamp. Neurons were injected with the current ramp following 20-min pretreatment with 0.1% DMSO ( $n = 6$ ) or 100 nM PMA ( $n = 5$ ). The ramp depolarized the membrane potential with a time course that essentially corresponded to the duration of the current injection. Subsequent to the current, the membrane potential did not recover to baseline but rather underwent a phase of prolonged depolarization (Fig. 10*A*). The extent of the peak depolarization evoked during the current injection itself was not different in DMSO versus PMA. (Fig. 10*B*). However, the prolonged depolarization elicited after the current was significantly larger following activation of PKC by PMA (Fig. 10*A*, right, and *C*) compared with DMSO (Fig. 10*A*, left, and *C*).

DISCUSSION

$\text{Ca}^{2+}$  channels hold a privileged position of triggering plasticity and secretion (Mermelstein et al. 2001; Neher and

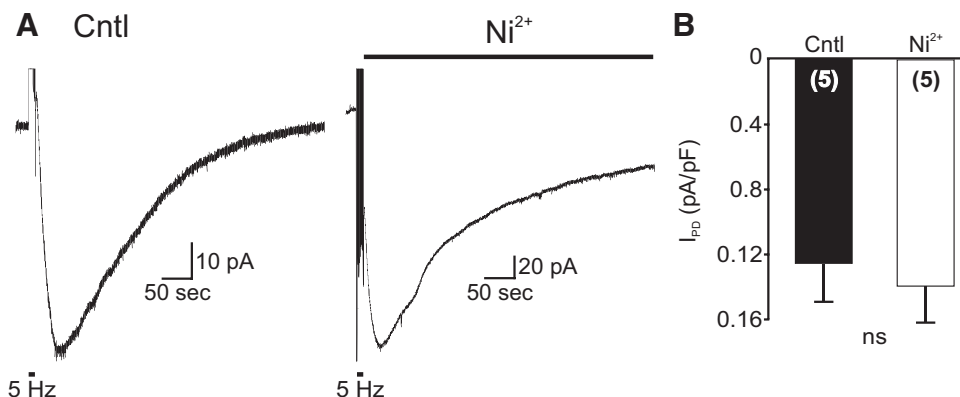


FIG. 6.  $\text{Ni}^{2+}$  does not inhibit the prolonged depolarization current. *A*, left: sample trace of prolonged depolarization current ( $I_{PD}$ ) evoked (at bar) with a 5-Hz, 10-s train of 100-ms pulses to  $+10$  mV from a holding potential of  $-60$  mV. The external is nASW while the pipette is filled with a  $\text{K}^+$ -aspartate-based solution. Right: sample trace of  $I_{PD}$ , but with 10 mM  $\text{Ni}^{2+}$  perfused onto the neuron just after the train.  $\text{Ni}^{2+}$  does not block the prolonged depolarization current. *B*: summary graph of peak  $I_{PD}$ , normalized to cell capacitance, elicited in the presence or absence of  $\text{Ni}^{2+}$ . The difference between the means is not significant (ns, 2-tailed unpaired Student's *t*-test).

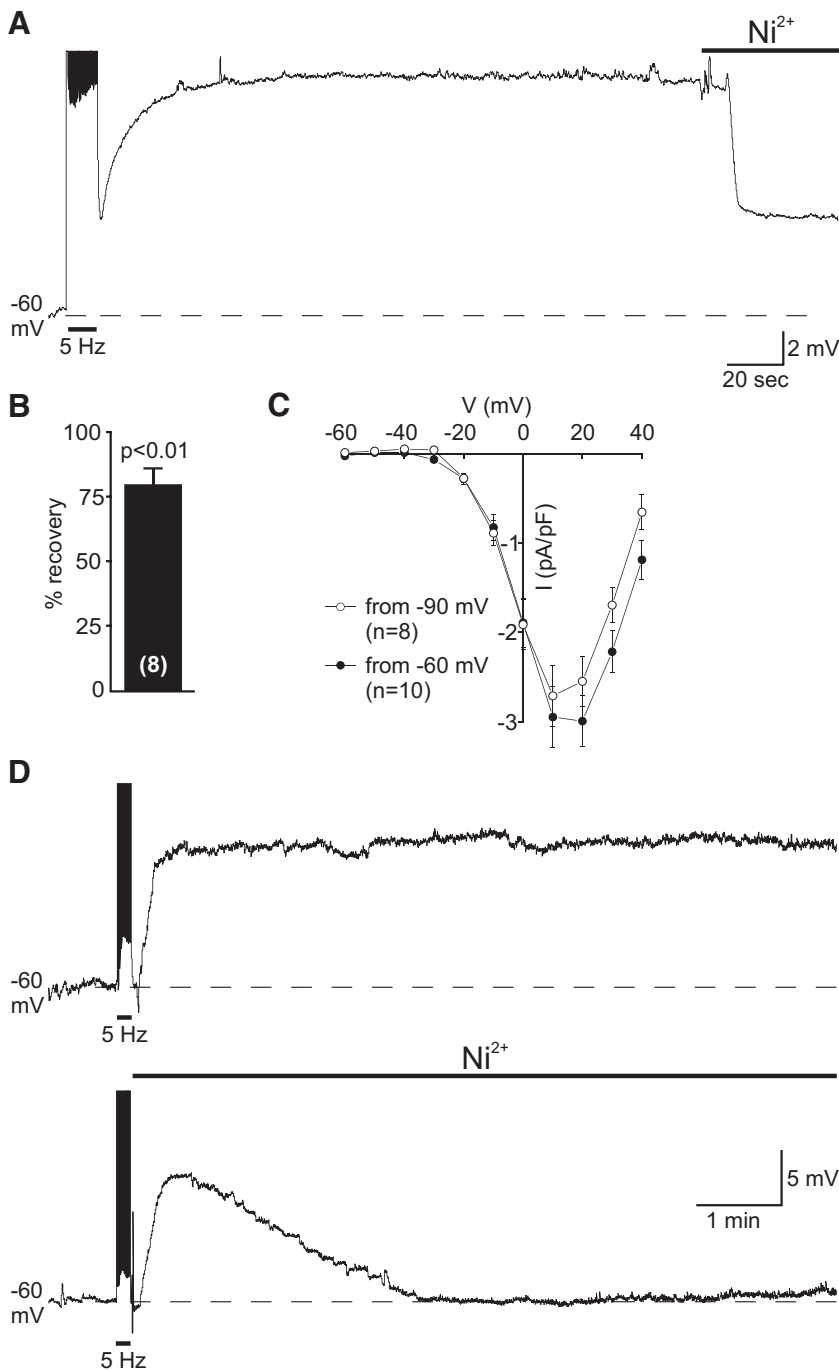


FIG. 7.  $\text{Ni}^{2+}$  inhibits an ongoing prolonged depolarization. *A*: sample trace of a prolonged depolarization, recorded in nASW with a  $\text{K}^+$ -acetate filled sharp electrode, evoked (at bar) with a 5-Hz, 10-s train of action potentials. Addition of 10 mM  $\text{Ni}^{2+}$  after the depolarization had plateaued leads to a reduction of the response. *B*: summary graph of percentage recovery back to baseline ( $-60$  mV) after perfusion of  $\text{Ni}^{2+}$ . The recovery is significant compared with a mean of 0 ( $*P < 0.01$ , 2-tailed 1-sample *t*-test). *C*: summary of peak  $\text{Ca}^{2+}$  current normalized to capacitance evoked by 200-ms square pulses from  $-60$  mV ( $\bullet$ ) or  $-90$  mV ( $\circ$ ). The 2 current-voltage relationships are very similar; in particular, there is a no plateau of over the negative test potentials when the neurons are held at  $-90$  mV. A T-type  $\text{Ca}^{2+}$  current would manifest as additional inward current activating at some point between  $-60$  and  $-20$  mV. *D*, *top*: control prolonged depolarization evoked by a train under sharp-electrode current-clamp shows little recovery over the duration of the recording period. Representative of  $n = 8$ . *Bottom*: when 10 mM  $\text{Ni}^{2+}$  is applied (at bar) just after the stimulus has ended, the response still occurs but does not remain in the depolarized state. Instead, the membrane potential recovers over the course of several minutes. Representative of  $n = 8$ .

Sakaba 2008) as well as passing inward current to affect excitability and activity (Eckert and Lux 1976; Metz et al. 2005; Wang et al. 2001). The bag cell neuron action potential is  $\text{Ca}^{2+}$  dependent with the upstroke mediated by a rapid  $\text{Ca}^{2+}$  channel designated as  $\text{Apl-Ca}_v1$ -based on partial cloning of the  $\alpha$ -subunit (Acosta-Urquidi and Dudek 1981; Kaczmarek and Stumwasser 1984; White and Kaczmarek 1997). PKC activity is upregulated  $\sim 5$  min into the afterdischarge (Wayne et al. 1999), which brings about the membrane insertion of a second species of rapid  $\text{Ca}^{2+}$  channel, known as  $\text{Apl-Ca}_v2$ , to increase macroscopic  $\text{Ca}^{2+}$  current (DeRiemer et al. 1985b; Zhang et al. 2008). These two currents have a similar voltage dependence, are weakly sensitive to nifedipine, and are blocked by milli-

molar levels of  $\text{Ni}^{2+}$ ,  $\text{Co}^{2+}$ , or  $\text{La}^{3+}$  (Hung and Magoski 2007; Strong et al. 1987). We now show that the bag cell neurons also express a persistent  $\text{Ca}^{2+}$  current.

Both the rapid and persistent  $\text{Ca}^{2+}$  current are enhanced when  $\text{Ba}^{2+}$  replaces  $\text{Ca}^{2+}$  as the charge carrier. This effect is widely reported for other  $\text{Ca}^{2+}$ -permeable channels (Friel and Tsien 1989; Geiger et al. 2009; Hagiwara et al. 1974; Hess et al. 1986; Tillotson 1979; Yue and Marban 1990).  $\text{Ba}^{2+}$  is believed to have a lower binding affinity than  $\text{Ca}^{2+}$  for the pore, resulting in greater mobility and conductance. In part, the larger rapid and persistent  $\text{Ba}^{2+}$  currents observed in the present study may arise from a prominent left-shift in activation. Byerly et al. (1985) reported a near  $-15$  mV shift in the  $V_{1/2}$  of activation

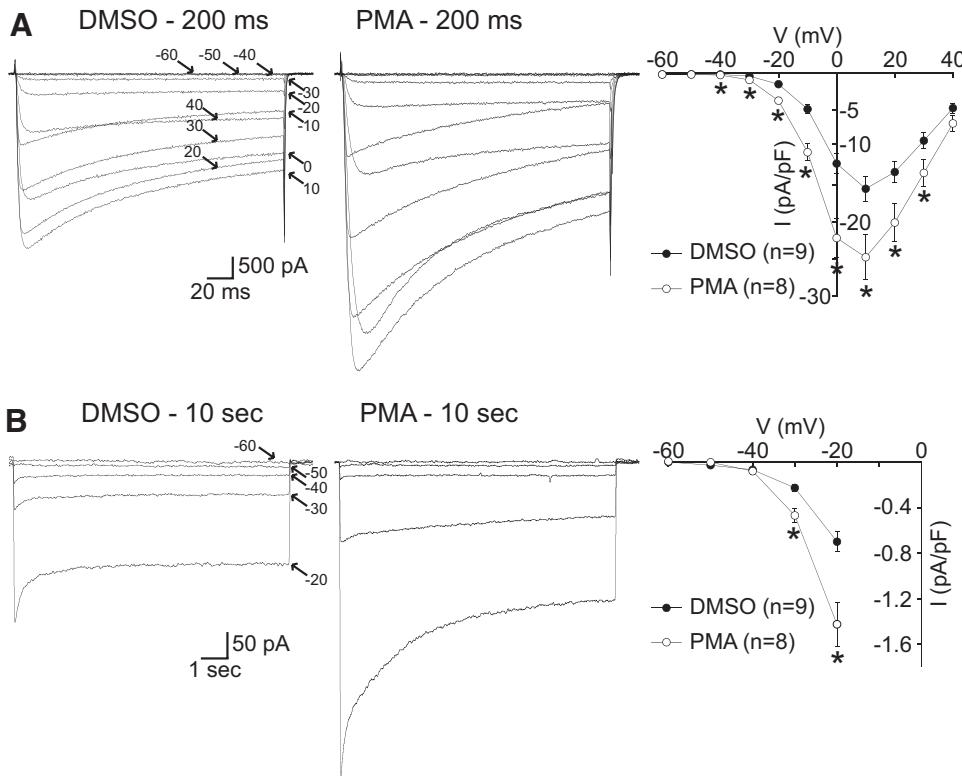


FIG. 8. PKC activation enhances both rapid and persistent  $\text{Ca}^{2+}$  current. *A, left*: traces of  $\text{Ca}^{2+}$  currents evoked by 200-ms square pulses from a holding potential of  $-60$  to  $+40$  mV in 10-mV increments following pretreatment in 0.1% DMSO for 30 min. *Middle*: traces of  $\text{Ca}^{2+}$  currents evoked from a different neuron following pretreatment in 100 nM PMA for 30 min. Scale bars apply to both panels. *Right*: summary graph of mean peak current elicited in the presence and absence of phorbol 12-myristate 13-acetate (PMA). The difference in peak current between the 2 conditions is significant at all voltages except  $-60$ ,  $-50$ , and  $+40$  mV ( $*P < 0.05$ , 1-tailed unpaired Student's *t*-test; Welch corrected for  $-10$  mV). *B, left*: traces of  $\text{Ca}^{2+}$  currents evoked by 10-s square pulses from  $-60$  to  $-20$  mV in 10-mV increments following pretreatment in 0.1% DMSO for 30 min. *Middle*: traces of  $\text{Ca}^{2+}$  currents evoked from a different neuron following pretreatment in 100 nM PMA for 30 min. Scale bars apply to both panels. *Right*: summary graph of persistent current, taken as the mean of the last 1 s, elicited in the presence and absence of PMA. The difference between the 2 conditions is significant at  $-30$  and  $-20$  mV ( $*P < 0.05$ , 1-tailed unpaired Student's *t*-test; Welch corrected for  $-20$  mV).

when using  $\text{Ba}^{2+}$  to record rapid  $\text{Ca}^{2+}$  currents from *Lymnaea* neurons. They suggested that  $\text{Ba}^{2+}$  impacts the voltage sensor by changing the external surface potential imposed on the channel. Regarding bag cell neurons, currents recorded by Fieber (1995), using  $\text{Ba}^{2+}$  as a charge carrier and a CsCl-based internal, show an inactivation  $V_{1/2}$  of  $-30$  mV; however, that study did not address activation nor did it assess the current with  $\text{Ca}^{2+}$  as charge carrier.

We confirmed that activation of bag cell neuron PKC increases the rapid  $\text{Ca}^{2+}$  current (DeRiemer et al. 1985b; Zhang et al. 2008). At the concentration used in the present study, PMA is a specific and potent activator of bag cell neuron PKC (DeRiemer et al. 1985a; Manseau et al. 2001). The enhanced  $\text{Ca}^{2+}$  current results in greater collective  $\text{Ca}^{2+}$  influx,  $\text{Ca}^{2+}$ -induced  $\text{Ca}^{2+}$  release, and peptide secretion during the after-discharge (Conn et al. 1989; Geiger and Magoski 2008; Loechner et al. 1992; Strong et al. 1987; Wayne et al. 1998). PKC-dependent modulation of rapid  $\text{Ca}^{2+}$  current is well established in both invertebrate and vertebrate neurons (e.g.,

Dreijer and Kits 1995; Hammond et al. 1987; Yang and Tsien 1993). Indeed, the original report by DeRiemer et al. (1985b) on bag cell neurons was the first to demonstrate that PKC could alter  $\text{Ca}^{2+}$  channel function. We now show that PKC has a similar effect on persistent  $\text{Ca}^{2+}$  current with a near doubling of the density. There is little known regarding specific intracellular signaling molecules modulating persistent  $\text{Ca}^{2+}$  current, although activation of adrenergic and serotonin receptors regulates these channels in hippocampal, spinal, and stomato-gastric neurons (Cloues et al. 1997; Li et al. 2007; Perrier and Hounsgaard 2003; Zhang et al. 1995).

Application of  $\text{Ni}^{2+}$  completely abolishes both the rapid and persistent  $\text{Ca}^{2+}$  current in bag cell neurons. While millimolar concentrations of  $\text{Ni}^{2+}$  will block most  $\text{Ca}^{2+}$  channels (Byerly et al. 1985; McFarlane and Gilly 1998), that the two currents share  $\text{Ni}^{2+}$  sensitivity suggests at the very least a common origin. Unfortunately, there are no adequate pharmacological tools to differentiate between bag cell neuron  $\text{Ca}^{2+}$  currents (Gardam et al. 2008; Strong et al. 1987). Despite the lack of

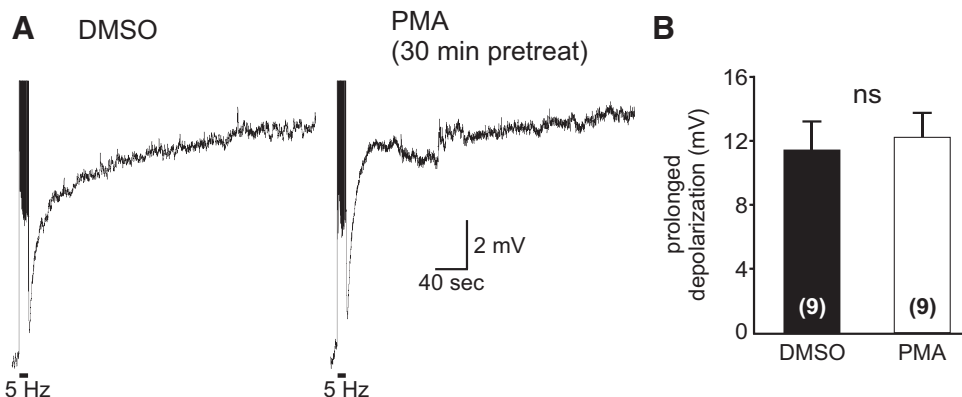


FIG. 9. Protein kinase C (PKC) activation does not alter the prolonged depolarization elicited by an action potential train. *A*: sample trace of prolonged depolarization evoked by a 5-Hz, 10-s train of action potentials following pretreatment with 0.1% DMSO (*left*) or a different neuron pretreated with 100 nM PMA for 20 min (*right*). The depolarization elicited by the train is essentially the same in either case. Scale bars apply to both panels. *B*: summary graph of mean prolonged depolarization with and without PMA pretreatment. The difference between the means is not significant (2-tailed unpaired Student's *t*-test).

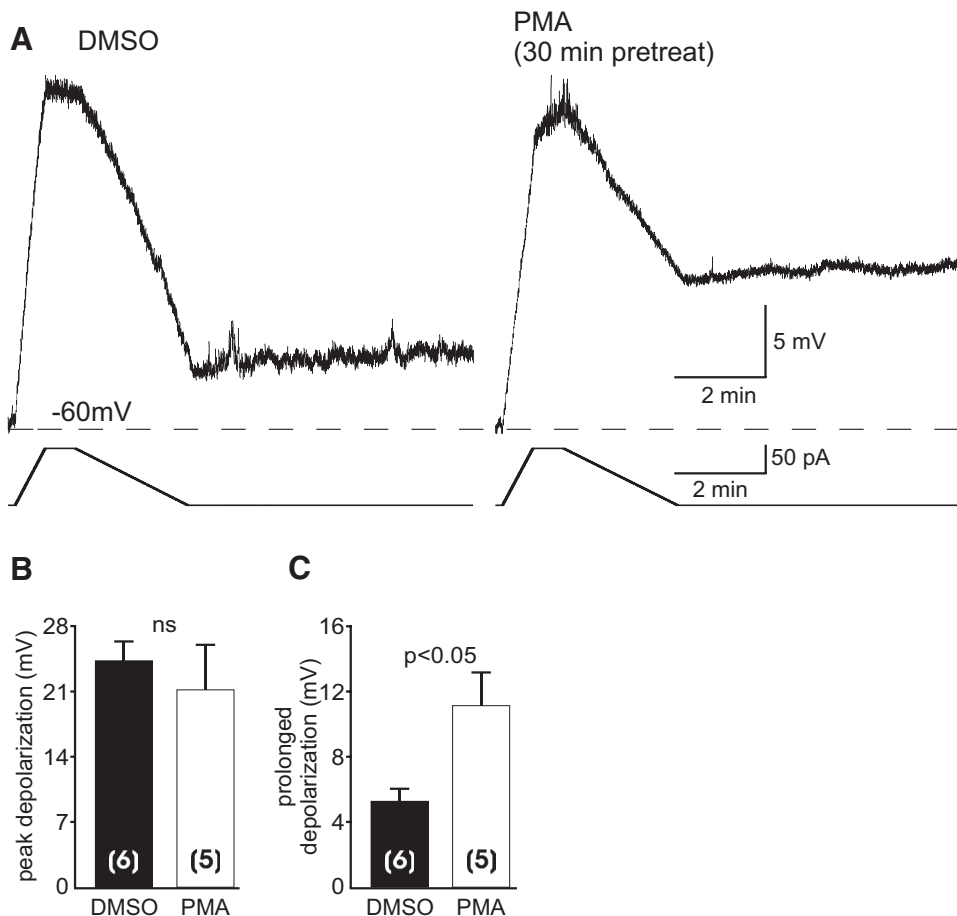


FIG. 10. PKC activation enhances prolonged depolarization elicited by a current ramp mimicking  $I_{PD}$ . **A**: sample trace of prolonged depolarization evoked after a current ramp in a neuron pretreated with 0.1% DMSO (*left*) or a different neuron pretreated with 100 nM PMA for 20 min (*right*). The ramp is an inverted idealized version of  $I_{PD}$ . The peak depolarization evoked during current injection is similar in both cases; however, the PMA pretreatment results in a larger prolonged depolarization elicited after the injection is turned off. Scale bars apply to both panels. **B**: summary graph of mean peak depolarization elicited by the ramp current shows that the mean response in control vs. PMA is not significantly different (2-tailed unpaired Student's *t*-test). **C**: summary graph of mean prolonged depolarization with and without PMA pretreatment. The difference between the means is significant (2-tailed unpaired Student's *t*-test; Welch corrected).

selectivity of  $Ni^{2+}$ , we have found it to be an effective blocker that avoids problems like altering the  $Na^+/Ca^{2+}$  exchanger or affecting  $K^+$  channels, which have been reported for  $Cd^{2+}$  and  $Co^{2+}$ , respectively (Agus et al. 1991; Le et al. 2005). This is important for experiments conducted under more physiological conditions, such as recording the prolonged depolarization in current-clamp. Moreover,  $Ni^{2+}$  does not alter  $I_{PD}$ , making it useful to distinguish between cation and  $Ca^{2+}$  currents.

The  $Ba^{2+}$  permeability, modulation by PKC, and  $Ni^{2+}$  block are consistent with the persistent  $Ca^{2+}$  current being the same species of channel that makes up the rapid  $Ca^{2+}$  current. How is it that a rapid current could generate a persistent current? There is a fair degree of overlap between the activation and inactivation curves for the rapid  $Ca^{2+}$  current, which in principle provides an opportunity for a "window current". Originally coined by Attwell et al. (1979) in reference to  $Na^+$  current, a window current is thought to be part of a fast, voltage-gated current that arises when the activation and inac-

tivation processes coincide with respect to voltage. Within this voltage range window, the channel undergoes a continuous cycle of transitioning from open to inactivated to closed, followed by re-opening (Cohen and Lederer 1987; Reuter and Scholz 1977). That stated, while the persistent  $Ca^{2+}$  current has a threshold between  $-50$  and  $-40$  mV, the amplitude of the prolonged depolarization can be as large as 15 mV but as small as 5 mV. This likely reflects a difference between the more physiological sharp-electrode current clamp, which does not appreciably alter the intracellular contents and uses nASW in the bath, and the less than physiological whole cell voltage-clamp, which replaces the intracellular contents with  $Cs^+$ -aspartate and uses  $Ca^{2+}$ - $Cs^+$ -TEA ASW in the bath. Thus the current flow observed in bag cell neurons between  $-50$  and  $-20$  mV under voltage clamp is likely physiological and would influence the membrane potential under current clamp. This is reinforced by our  $Ca^{2+}$ -imaging showing that even small depolarizations are capable of evoking  $Ca^{2+}$  influx in

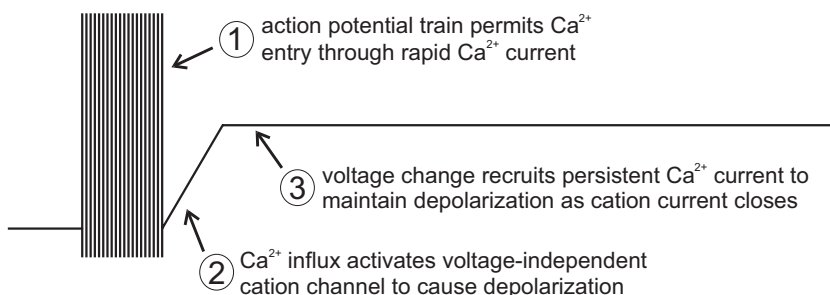


FIG. 11. The prolonged depolarization is determined by dynamic interactions between different conductances. Schematic of bag cell neuron membrane potential during a prolonged depolarization.  $Ca^{2+}$  entry via rapid, voltage-dependent  $Ca^{2+}$  current occurs during the action potential train (step 1). This increase in intracellular  $Ca^{2+}$  triggers a voltage-independent cation current that depolarizes the membrane and mediates the initial phase of the response. The positive change in membrane potential opens voltage-dependent persistent  $Ca^{2+}$  current to maintain the prolonged depolarization even as the cation current turns off (step 3).

normal extracellular medium, presumably by recruiting persistent  $\text{Ca}^{2+}$  current.

Typically, persistent  $\text{Ca}^{2+}$  current is ascribed to L-type  $\text{Ca}^{2+}$  channels, either characterized physiologically and/or pharmacologically in neurons and myocytes (Carlin et al. 2000a,b; Cohen and Lederer 1987; Fisher and Bourque 1995) or expressed in cell lines (McRory et al. 2004; Xu and Lipscombe 2001). In particular,  $\text{Ca}_v1.3$  and  $\text{Ca}_v1.4$  present activation thresholds that are within 10–20 mV of typical neuronal resting potentials and once open they inactivate very slowly. The extent that  $\text{Ca}^{2+}$ -dependent inactivation determines the steady-state amplitude of the bag cell neuron persistent  $\text{Ca}^{2+}$  current is unclear.  $\text{Ca}^{2+}$ -dependent inactivation in L-type channels is mediated by closely associated calmodulin (Zuhlke et al. 1999). This can be assessed by using  $\text{Ba}^{2+}$  as a charge carrier because it binds calmodulin poorly and lessens  $\text{Ca}^{2+}$ -dependent inactivation when passing through the channel (Chao et al. 1981; Tillotson 1979). However, similar to a report by McRory et al. (2004) on  $\text{Ca}_v1.4$ , we found that the inactivation of both fast and persistent bag cell neuron  $\text{Ca}^{2+}$  currents is not dramatically slowed by  $\text{Ba}^{2+}$ .

The bag cell neuron persistent  $\text{Ca}^{2+}$  current meets the criteria for a conductance that would act as a pacemaker current to maintain the membrane potential in an up-state, i.e., more positive than rest. However, to make this transition, the membrane potential must first be depolarized. Thus the  $\text{Ca}^{2+}$  current plays two roles in generating the prolonged depolarization: one, permitting substantial  $\text{Ca}^{2+}$  influx during the initial stimulus to activate the voltage-independent cation current ( $I_{\text{PD}}$ ) (Geiger and Magoski 2008; Hung and Magoski 2007); two, after the cation channel has brought the membrane potential into the threshold range of the  $\text{Ca}^{2+}$  current, the persistent mode then contributes steady-state inward current to promote the response (Fig. 11). In agreement with this, the duration of the depolarization is shortened when  $\text{Ni}^{2+}$  is introduced immediately after the train, whereas the magnitude of the response is suppressed when  $\text{Ni}^{2+}$  is applied once the prolonged depolarization is fully underway. Of course, we cannot rule out the possibility that some other current is a factor in the long-term effect on membrane potential. Given that the persistent current is by definition  $\text{Ca}^{2+}$  permeable,  $\text{Ca}^{2+}$  influx during the prolonged depolarization could trigger additional channels, including perhaps re-recruiting the cation current.

Neurons from the septal nucleus, stomatogastric ganglion, hippocampus, entorhinal cortex, *Aplysia* buccal ganglion, and lumbosacral spinal cord achieve activity-dependent change by employing  $\text{Ca}^{2+}$  current simply to deliver the requisite  $\text{Ca}^{2+}$  for cation channel opening (Dembrow et al. 2004; Derjean et al. 2005; Egorov et al. 2002; Fraser and MacVicar 1996; Hasuo et al. 1990; Zhang et al. 1995). Alternatively, dorsal horn, motor, *Manduca*, and suprachiasmatic neurons use persistent  $\text{Ca}^{2+}$  current exclusively for pacemaking (Carlin et al. 2000b; Kononenko and Dudek 2006; Lee and Heckman 1998; Mercer et al. 2005; Russo and Hounsgaard 1996). There are two prior studies, concerning plateau potentials, with some similarities to our findings. Specifically, in subthalamic nucleus and dorsal horn neurons the initial phase of depolarization is due to persistent  $\text{Ca}^{2+}$  current, which in turn elicits a cation current that carries the latter phase (Beurrier et al. 1999; Morisset and Nagy 1999). For the bag cell neuron-prolonged

depolarization, the interplay between  $\text{Ca}^{2+}$  and cation channel is a degree more sophisticated, requiring rapid  $\text{Ca}^{2+}$  current, then  $\text{Ca}^{2+}$ -activated cation current, followed by persistent  $\text{Ca}^{2+}$  current.

During an afterdischarge in the intact bag cell neuron cluster, the persistent current would contribute tonic inward current to maintain the neurons in a depolarized state necessary for action potential firing, the secretion of egg-laying hormone, and reproduction. The upregulation of PKC that occurs once the afterdischarge is underway (Wayne et al. 1999) could enhance both the rapid and persistent mode of the  $\text{Ca}^{2+}$  current, thus providing additional drive. Our work highlights how neurons in general may use interactions involving  $\text{Ca}^{2+}$  and cation channels to achieve long-term, activity-dependent changes in excitability with implications for the initiation of behavior.

#### ACKNOWLEDGMENTS

The authors thank S. L. Smith for technical assistance and N. M. Magoski for evaluation of previous drafts of the manuscript.

#### GRANTS

A.K.H. Tam held a Ruth Taylor Research Fund Scholarship from Queen's University and a Summer Studentship from Epilepsy Canada. A. Y. Hung held a Canadian Institutes of Health Research (CIHR) Canada Graduate Scholarship Master's Award, and N. S. Magoski holds a CIHR New Investigator Award. This work was supported by a CIHR operating grant to N. S. Magoski.

#### REFERENCES

- Acosta-Urquidí J, Dudek FE. Soma spike of neuroendocrine bag cells of *Aplysia californica*. *J Neurobiol* 12: 367–378, 1981.
- Agus ZS, Dukes ID, Morad M. Divalent cations modulate the transient outward current in rat ventricular myocytes. *Am J Physiol Cell Physiol* 261: C310–C318, 1991.
- Aizenman CD, Linden DJ. Rapid, synaptically driven increases in the intrinsic excitability of cerebellar deep nuclear neurons. *Nat Neurosci* 3: 109–111, 2000.
- Andrew RD, Dudek FE. Burst discharge in mammalian neuroendocrine cells involves an intrinsic regenerative mechanism. *Science* 221: 1050–1052, 1983.
- Attwell D, Cohen I, Eisner D, Ohba M, Ojeda C. The steady state TTX-sensitive (“window”) sodium current in cardiac Purkinje fibers. *Pfluegers* 379: 137–142, 1979.
- Beurrier C, Congar P, Bioulac B, Hammond C. Subthalamic nucleus neurons switch from single-spike activity to burst-firing mode. *J Neurosci* 19: 599–609, 1999.
- Brown CH, Bourque CW. Autocrine feedback inhibition of plateau potentials terminates phasic bursts in magnocellular neurosecretory cells of the rat supraoptic nucleus. *J Physiol* 557: 949–960, 2004.
- Byerly L, Chase BP, Stimers JR. Permeation and interaction of divalent cations in calcium channels of snail neurons. *J Gen Physiol* 85: 491–518, 1985.
- Carbone E, Lux HD. A low voltage-activated, fully inactivating Ca channel in vertebrate sensory neurones. *Nature* 310: 501–502, 1984.
- Carlin KP, Jiang Z, Brownstone RM. Characterization of calcium currents in functionally mature mouse spinal motoneurons. *Eur J Neurosci* 12: 1624–1634, 2000a.
- Carlin KP, Jones KE, Jiang Z, Jordan LM, Brownstone RM. Dendritic L-type calcium currents in mouse spinal motoneurons: implications for bistability. *Eur J Neurosci* 12: 1635–1646, 2000b.
- Castagna M, Takai Y, Kaibuchi K, Sano K, Kikkawa U, Nishizuka Y. Direct activation of calcium-activated, phospholipid-dependent protein kinase by tumor-promoting phorbol esters. *J Biol Chem* 257: 7847–7851, 1982.
- Chao S-H, Suzuki Y, Zysk JR, Cheung WY. Activation of calmodulin by various metal cations as a function of ionic radius. *Mol Pharmacol* 26: 75–82, 1984.
- Chiu AY, Hunkapiller MW, Heller E, Stuart DK, Hood LE, Strumwasser F. Purification and primary structure of the neuropeptide egg-laying hormone of *Aplysia californica*. *Proc Natl Acad Sci USA* 76: 6656–6660, 1979.

- Cloues RK, Tavalin SJ, Marrion NV.**  $\beta$ -adrenergic stimulation selectively inhibits long-lasting L-type calcium channel facilitation in hippocampal pyramidal neurons. *J Neurosci* 17: 6493–6503, 1997.
- Cohen NM, Lederer WJ.** Calcium current in isolated neonatal rat ventricular myocytes. *J Physiol* 391: 169–191, 1987.
- Conn PJ, Strong JA, Kaczmarek LK.** Inhibitors of protein kinase C prevent enhancement of calcium current and action potentials in peptidergic neurons of *Aplysia*. *J Neuroscience* 9: 480–487, 1989.
- Dembrow NC, Jing J, Brezina V, Weiss KR.** A specific synaptic pathway activates a conditional plateau potential underlying protraction phase in the *Aplysia* feeding central pattern generator. *J Neurosci* 24: 5230–5238, 2004.
- DeRiemer SA, Greengard P, Kaczmarek LK.** Calcium/phosphatidylserine/diacylglycerol-dependent protein phosphorylation in the *Aplysia* nervous system. *J Neurosci* 5: 2672–2676, 1985a.
- DeRiemer SA, Strong JA, Albert KA, Greengard P, Kaczmarek LK.** Enhancement of calcium current in *Aplysia* neurons by phorbol ester and protein kinase C. *Nature* 313: 313–316, 1985b.
- Derjean D, Bertrand S, Nagy F, Scefchyk SJ.** Plateau potentials and membrane oscillations in parasympathetic preganglionic neurons and intermedialateral neurons in the rat lumbosacral spinal cord. *J Physiol* 563: 583–596, 2005.
- Dreijer AMC, Kits KS.** Multiple second messenger routes enhance two high-voltage-activated calcium currents in molluscan neuroendocrine cells. *Neuroscience* 64: 787–800, 1995.
- Eckert R, Lux HD.** A voltage-sensitive persistent calcium conductance in neuronal somata of *Helix*. *J Physiol* 254: 129–151, 1976.
- Egorov AV, Hamam BN, Fransén E, Hasselmo ME, Alonso AA.** Graded persistent activity in entorhinal cortex neurons. *Nature* 420: 173–178, 2002.
- Eyzaguirre C, Kuffler SW.** Processes of excitation in the dendrites and in the soma of single isolated sensory nerve cells of the lobster and crayfish. *J Gen Physiol* 39: 87–119, 1955.
- Fieber LA.** Characterization and modulation of  $\text{Na}^+$  and  $\text{Ca}^{2+}$  currents underlying the action potential in bag cells of two species of *Aplysia*. *J Exp Biol* 198: 2337–2347, 1995.
- Fisher TE, Bourque CW.** Voltage-gated calcium currents in the magnocellular neurosecretory cells of the rat supraoptic nucleus. *J Physiol* 486: 571–580, 1995.
- Fox AP, Nowycky MC, Tsien RW.** Kinetic and pharmacological properties distinguishing three types of calcium currents in chick sensory neurons. *J Physiol* 394: 149–172, 1987.
- Friel DD, Tsien RW.** Voltage-gated calcium channels: direct observation of the anomalous mole fraction effect at the single-channel level. *Proc Natl Acad Sci USA* 86: 5207–5211, 1989.
- Fraser DD, MacVicar BA.** Cholinergic-dependent plateau potential in hippocampal CA1 pyramidal neurons. *J Neurosci* 16: 4113–4128, 1996.
- Gardam KE, Geiger JE, Hickey CM, Hung AY, Magoski NS.** Flufenamic acid affects multiple currents and causes intracellular  $\text{Ca}^{2+}$  release in *Aplysia* bag cell neurons. *J Neurophysiol* 100: 38–49, 2008.
- Gardam KE, Magoski NS.** Regulation of cation channel voltage and  $\text{Ca}^{2+}$  dependence by multiple modulators. *J Neurophysiol* 102: 259–271, 2009.
- Geiger JE, Magoski NS.**  $\text{Ca}^{2+}$ -induced  $\text{Ca}^{2+}$  release in *Aplysia* bag cell neurons requires interaction between mitochondrial and endoplasmic reticulum stores. *J Neurophysiol* 100: 24–37, 2008.
- Geiger JE, Hickey CM, Magoski NS.**  $\text{Ca}^{2+}$  entry through a non-selective cation channel in *Aplysia* bag cell neurons. *Neuroscience* 162: 1023–1038, 2009.
- Hagiwara S, Fukuda J, Eaton DC.** Membrane currents carried by Ca, Sr, and Ba in barnacle muscle fiber during voltage clamp. *J Gen Physiol* 63: 564–578, 1974.
- Hammond C, Paupardin-Tritsch D, Nairn AC, Greengard P, Gershenfeld HM.** Cholecystokinin induces a decrease in  $\text{Ca}^{2+}$  current in snail neurons that appears to be mediated by protein kinase C. *Nature* 325: 809–811, 1987.
- Hasuo H, Phelan KD, Twery MJ, Gallagher JP.** A calcium-dependent slow afterdepolarization recorded in rat dorsolateral septal nucleus neurons in vitro. *J Neurophysiol* 64: 1838–1846, 1990.
- Hess P, Lansman JB, Tsien RW.** Calcium channel selectivity for divalent and monovalent cations. Voltage and concentration dependence of single channel current in ventricular heart cells. *J Gen Physiol* 88: 293–319, 1986.
- Hille B.** *Ionic Channels of Excitable Membranes*. Sunderland, MA: Sinauer, 2001.
- Hung AY, Magoski NS.** Activity-dependent initiation of a prolonged depolarization in *Aplysia* bag cell neurons: role for a cation channel. *J Neurophysiol* 97: 2465–2479, 2007.
- Kaczmarek LK, Jennings K, Strumwasser F.** An early sodium and a late calcium phase in the afterdischarge of peptide-secreting neurons of *Aplysia*. *Brain Res* 238: 105–115, 1982.
- Kaczmarek LK, Strumwasser F.** A voltage-clamp analysis of currents in isolated peptidergic neurons of *Aplysia*. *J Neurophysiol* 52: 340–349, 1984.
- Kononenko NI, Dudek FE.** Persistent calcium current in rat suprachiasmatic nucleus neurons. *Neuroscience* 138: 377–388, 2006.
- Kupfermann I.** Stimulation of egg laying: possible neuroendocrine function of bag cells of abdominal ganglion of *Aplysia californica*. *Nature* 216: 814–815, 1967.
- Kupfermann I, Kandel ER.** Electrophysiological properties and functional interconnections of two symmetrical neurosecretory clusters (bag cells) in abdominal ganglion of *Aplysia*. *J Neurophysiol* 33: 865–876, 1970.
- Le HD, Omelchenko A, Hryshko LV, Uliyanova A, Condrescu M, Reeves JP.** Allosteric activation of sodium–calcium exchange by picomolar concentrations of cadmium. *J Physiol* 563: 105–117, 2005.
- Lee JH, Gomora JC, Cribbs LL, Perez-Reyes E.** Nickel block of three T-type calcium channels: low concentrations selectively block  $\alpha 1\text{H}$ . *Biophys J* 77: 3034–3042, 1999.
- Lee RH, Heckman CJ.** Bistability in spinal motoneurons in vivo: systematic variations in persistent inward currents. *J Neurophysiol* 80: 583–593, 1998.
- Li X, Murray K, Harvey PJ, Ballou EW, Bennett DJ.** Serotonin facilitates a persistent calcium current in motoneurons of rats with and without chronic spinal cord injury. *J Neurophysiol* 97: 1236–1246, 2007.
- Loechner KJ, Mattessich-Arrandale J, Azhderian EM, Kaczmarek LK.** Inhibition of peptide release from invertebrate neurons by the protein kinase inhibitor H7. *Brain Res* 581: 315–318, 1992.
- Lupinsky DA, Magoski NS.**  $\text{Ca}^{2+}$ -dependent regulation of a non-selective cation channel from *Aplysia* bag cell neurons. *J Physiol* 575: 491–506, 2006.
- Magoski NS, Kaczmarek LK.** Association/Dissociation of a channel-kinase complex underlies state-dependent modulation. *J Neurosci* 25: 8037–8047, 2005.
- Manseau F, Fan X, Hueftlein T, Sossin WS, Castellucci VF.**  $\text{Ca}^{2+}$ -independent protein kinase C AplIII mediates the serotonin-induced facilitation at depressed *Aplysia* sensorimotor synapses. *J Neurosci* 21: 1247–1256, 2001.
- McFarlane MB, Gilly WF.** State-dependent nickel block of a high-voltage-activated neuronal calcium channel. *J Neurophysiol* 80: 1678–1685, 1998.
- McRory JE, Hamid J, Doering CJ, Garcia E, Parker R, Hamming K, Chen L, Hildebrand M, Beedle AM, Feldcamp L, Zamponi GW, Snutch TP.** The *CACNA1F* gene encodes an L-type calcium channel with unique biophysical properties and tissue distribution. *J Neurosci* 24: 1707–1718, 2004.
- Mercer AR, Kloppenburg P, Hildebrand JG.** Plateau potentials in developing antennal-lobe neurons of the moth, *Manduca sexta*. *J Neurophysiol* 93: 1949–1958, 2005.
- Mermelstein PG, Deisseroth K, Dasgupta N, Isaksen AL, Tsien RW.** Calmodulin priming: nuclear translocation of a calmodulin complex and the memory of prior neuronal activity. *Proc Natl Acad Sci USA* 98: 15342–15347, 2001.
- Morisset V, Nagy F.** Ionic basis for plateau potentials in deep dorsal horn neurons of the rat spinal cord. *J Neurosci* 19: 7309–7316, 1999.
- Metz AE, Jarsky T, Martina M, Spruston S.** R-type calcium channels contribute to afterdepolarization and bursting in hippocampal CA1 pyramidal neurons. *J Neurosci* 25: 5763–5773, 2005.
- Neher E, Sakaba T.** Multiple roles of calcium ions in the regulation of neurotransmitter release. *Neuron* 59: 861–872, 2008.
- Nelson AB, Gittis AH, du Lac S.** Decreases in CaMKII activity trigger persistent potentiation of intrinsic excitability in spontaneously firing vestibular nucleus neurons. *Neuron* 46: 623–631, 2005.
- Perrier J-F, Hounsgaard J.** 5-HT<sub>2</sub> receptors promote plateau potentials in turtle spinal motoneurons by facilitating an L-type calcium current. *J Neurophysiol* 89: 954–959, 2003.
- Pinsker HM, Dudek FE.** Bag cell control of egg laying in freely behaving *Aplysia*. *Science* 197: 490–493, 1977.
- Rekling JC, Feldman JL.** Calcium-dependent plateau potentials in rostral ambiguous neurons in the newborn mouse brain stem in vitro. *J Neurophysiol* 78: 2483–2492, 1997.
- Reuter H, Scholz H.** A study of the ion selectivity and the kinetic properties of the calcium dependent slow inward current in mammalian cardiac muscle. *J Physiol* 264: 17–47, 1977.
- Russell DF, Hartline DK.** Slow active potentials and bursting motor patterns in pyloric network of the lobster, *Panulirus interruptus*. *J Neurophysiol* 48: 914–937, 1982.

- Russo RE, Hounsgaard J.** Plateau-generating neurons in the dorsal horn in an in vitro preparation of the turtle spinal cord. *J Physiol* 493: 39–54, 1996.
- Soto-Trevino C, Thoroughman KA, Marder E, Abbott LF.** Activity-dependent modification of inhibitory synapses in models of rhythmic neural networks. *Nat Neurosci* 4: 297–303, 2001.
- Strong JA, Fox AP, Tsien RW, Kaczmarek LK.** Stimulation of protein kinase C recruits covert calcium channels in *Aplysia* bag cell neurons. *Nature* 325: 714–717, 1987.
- Stuart DK, Chiu AY, Strumwasser F.** Neurosecretion of egg-laying hormone and other peptides from electrically active bag cell neurons of *Aplysia*. *J Neurophysiol* 43: 488–498, 1980.
- Tasaki I, Polley EH, Orrego F.** Action potentials from individual elements in cat geniculate and striate cortex. *J Neurophysiol* 17: 454–474, 1954.
- Teruyama R, Armstrong WE.** Enhancement of calcium-dependent afterpotentials in oxytocin neurons of the rat supraoptic nucleus during lactation. *J Physiol* 566: 505–518, 2005.
- Tillotson D.** Inactivation of  $\text{Ca}^{2+}$  conductance dependent on entry of  $\text{Ca}^{2+}$  ions in molluscan neurons. *Proc Natl Acad Sci USA* 76: 1497–1500, 1979.
- Thompson SH, Smith SJ.** Depolarizing afterpotentials and burst production in molluscan pacemaker neurons. *J Neurophysiol* 39: 153–61, 1976.
- Viana Di Prisco G, Pearlstein E, Robitaille R, Dubuc R.** Role of sensory-evoked NMDA plateau potentials in the initiation of locomotion. *Science* 278: 1122–1125, 1997.
- Vorndran C, Minta A, Poenie M.** New fluorescent calcium indicators designed for cytosolic retention or measuring calcium near membranes. *Biophys J* 69: 2112–2124, 1995.
- Wang JW, Denk W, Flores J, Gelperin A.** Initiation and propagation of calcium-dependent action potentials in a coupled network of olfactory interneurons. *J Neurophysiol* 85: 977–985, 2001.
- Wayne NL, Kim YJ, Yong-Montenegro RJ.** Seasonal fluctuations in the secretory response of neuroendocrine cells of *Aplysia californica* to inhibitors of protein kinase A and protein kinase C. *Gen Comp Endocrinol* 109: 356–365, 1998.
- Wayne NL, Lee W, Kim YJ.** Persistent activation of calcium-activated and calcium-independent protein kinase C in response to electrical afterdischarge from peptidergic neurons of *Aplysia*. *Brain Res* 834: 211–213, 1999.
- Whim MD, Kaczmarek LK.** Heterologous expression of the Kv3.1 potassium channel eliminates spike broadening and the induction of a depolarizing afterpotential in the peptidergic bag cell neurons. *J Neurosci* 18: 9171–9180, 1998.
- White BH, Kaczmarek LK.** Identification of a vesicular pool of calcium channels in the bag cell neurons of *Aplysia californica*. *J Neurosci* 17: 1582–1595, 1997.
- Wilson WA, Wachtel H.** Negative resistance characteristic essential for the maintenance of slow oscillations in bursting neurons. *Science* 186: 932–934, 1974.
- Wilson GF, Richardson FC, Fisher TE, Olivera BM, Kaczmarek LK.** Identification and characterization of a  $\text{Ca}^{2+}$ -sensitive nonspecific cation channel underlying prolonged repetitive firing in *Aplysia* neurons. *J Neurosci* 16: 3661–3671, 1996.
- Xu W, Lipscombe D.** Neuronal  $\text{Ca}_v1.3$  L-type channels activate at relatively hyperpolarized membrane potentials and are incompletely inhibited by dihydropyridines. *J Neurosci* 21: 5944–5951, 2001.
- Yang J, Tsien RW.** Enhancement of N- and L-type calcium currents by protein kinase C in frog sympathetic neurons. *Neuron* 10: 127–136, 1993.
- Yeoman MS, Brezden BL, Benjamin PR.** LVA and HVA  $\text{Ca}^{2+}$  currents in ventricular muscle cells of the *Lymnaea* heart. *J Neurophysiol* 82: 2428–2440, 1999.
- Yue DT, Marban E.** Permeation in the dihydropyridine-sensitive calcium channel. Multi-ion occupancy but no anomalous mole-fraction effect between  $\text{Ba}^{2+}$  and  $\text{Ca}^{2+}$ . *J Gen Physiol* 95: 911–939, 1990.
- Zhang B, Harris-Warrick RM.** Calcium-dependent plateau potentials in a crab stomatogastric ganglion motor neuron. I. Calcium current and its modulation by serotonin. *J Neurophysiol* 74: 1929–1937, 1995.
- Zhang B, Wootton JF, Harris-Warrick RM.** Calcium-dependent plateau potentials in a crab stomatogastric ganglion motor neuron. II. Calcium-activated slow inward current. *J Neurophysiol* 74: 1938–1946, 1995.
- Zhang Y, Helm JS, Senatore A, Spafford JD, Kaczmarek LK, Jonas EA.** PKC-induced intracellular trafficking of  $\text{Ca}_v2$  precedes its rapid recruitment to the plasma membrane. *J Neurosci* 28: 2601–2612, 2008.
- Zuhlke RD, Pitt GS, Deisseroth K, Tsien RW, Reuter H.** Calmodulin supports both inactivation and facilitation of L-type calcium channels. *Nature* 399: 159–162, 1999.